

# Thermal remote sensing for reservoir modelling and management

Belén Martí-Cardona<sup>(1,2)</sup>, Marina Arbat-Bofill<sup>(2)</sup>, Jordi Prats-Rodríguez<sup>(3,2)</sup>, Luca Pipia<sup>(4)</sup>

<sup>(1)</sup> *Dep. of Civil and Env. Eng., Un. of Surrey, 29AA03, Guildford, GU2 7XH, U.K., b.marti-cardona@surrey.ac.uk*

<sup>(2)</sup> *Institut Flumen, Un. Politècnica de Catalunya, Jordi Girona 1 D1, 08034 Barcelona, Spain, marina.arbat@upc.edu*

<sup>(3)</sup> *IRSTEA, 3275 Route Cézanne, 13100 Aix-en-Provence, France, jordi.prats@irstea.fr*

<sup>(4)</sup> *Institut Cartogràfic i Geològic de Catalunya, Parc de Montjuïc s/n, 08038 Barcelona, Spain, luca.pipia@icgc.cat*

## ABSTRACT

ASTER and Landsat images were used for mapping the water surface temperature in the Sobrón, Mequinenza and Ribarroja reservoirs in the Ebro River, Spain. The spatially continuous information in these maps reveals the impact of the reservoir on the river natural thermal gradient in two different periods of the year. It also evidences the thermal impact intensity and extent of the refrigeration flow discharge from a nuclear power plant located on the river bank.

The high spatial resolution images of the Ribarroja reservoir, acquired by the airborne hyperspectral TASI sensor, show spatial patterns which complemented the in-situ point measurements and contributed valuable data for validating the three-dimensional thermo-hydrodynamic model of the reservoir.

## 1. INTRODUCTION

The presence of reservoirs has a great impact on the rivers natural thermal regime [1]. This impact is exacerbated by the climate warming trend and by the use of the river flow for refrigeration in power plants. Water temperature variations affect the reservoir hydrodynamics, water quality, and the aquatic ecosystem functioning within and downstream the reservoir. Modelling the thermal behaviour of reservoirs allows assessing their response to changing climate conditions and operation actions, thus assisting their management.

During the last two decades several studies investigated the thermal behaviour of the Ebro River, in North East Spain, and the impact of the reservoirs and power plants along its course [1], [2], [3]. These studies included the acquisition of continuous in-depth water temperatures for certain periods in several reservoirs. In recent years, the in-situ measurements have been supplemented with the spatial information on surface water temperature obtained from satellite and airborne imagery. Additionally, numerical models have been developed for the simulation of water temperature under different ambient conditions or reservoir operation hypothesis in order to assist their management.

This article describes the findings derived from the use

of remote sensing data regarding the reservoir thermal behaviour and its impact on the fluvial system, for the Sobrón, Mequinenza and Ribarroja reservoirs. It also shows how the thermal data contributed to validate a numerical water temperature simulation model. The article highlights the additional insight on the fluvial thermodynamic processes provided by the image spatially continuous data over large areas and its complementarity with point in-depth measurements.

## 2. STUDY AREA

The study area encompasses three reservoirs in the Ebro River, Spain, namely: Sobrón, Mequinenza and Ribarroja. Fig. 1 indicates the location of the reservoirs.

Special attention is paid to the confluence of the Segre tributary into the tail of the Ribarroja reservoir, approximately 1 km downstream of the Mequinenza dam (Fig. 1). In this site, flow discharges with different characteristics come together and complex mixing phenomena take place.

During the summer, the main incoming heat in the reservoir is the solar radiation striking the water surface. This results in the formation of a vertical gradient, with water getting colder and denser with depth. This situation, known as thermal stratification, confers great stability to the water body. The Ebro River reaches the thermally stratified Mequinenza reservoir at a lower temperature than the impounded water surface, and flows into the water body at the matching density depth. In the Mequinenza dam, water is discharged from the reservoir bottom for hydroelectric power generation. The profound waters submerge under the warmer surface water of the downstream Ribarroja reservoir.

In autumn and winter, the cooling of the reservoir surface promotes the breakdown of the stratification and the water vertical mixing. Due to its greater thermal inertia, the impounded Mequinenza and Ribarroja waters cool down and warm up at a slower pace than the Ebro River.

The Sobrón reservoir is also located in the Ebro River, approximately 200 km upstream of Mequinenza. On the right bank of a pronounced meander, at the tail of the

reservoir, there is a nuclear power plant which was operative from 1962 until 2012. The plant used to take water from the river for the refrigeration of the reactor, which was then discharged at the reservoir tail, as indicated in Fig. 1. In past years, some environmental concerns aroused regarding the possible excessive heating of the reservoir due to the plant's cooling flow discharge.

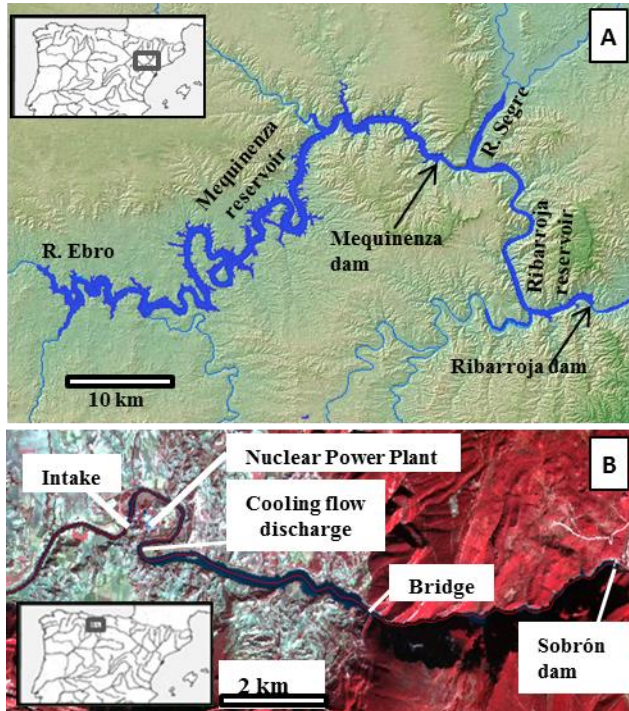


Figure 1. Location of a) the Mequinenza and Ribarroja reservoirs and b) Sobrón reservoir, on a false color ASTER image.

### 3. EXPERIMENTAL DATA AND METHODOLOGY

#### 3.1. Remote sensing data

The work presented in this document was undertaken as part of an on-going study, in which data from the following satellite sensors has been utilised: Terra/ASTER, Landsat 5/TM and Landsat 8/OLI, TIRS. Additionally, three data acquisition campaigns were carried out with the TASI hyperspectral sensor on board a piloted aircraft and a NEC F30 microbolometer camera on an unmanned airborne vehicle. This article includes results from the remote sensing data indicated in Tab. 1.

##### *Mequinenza and Ribarroja reservoirs*

The ASTER images of Mequinenza and Ribarroja reservoir were acquired in the September and March, at the end of the summer and winter seasons, moments in which the impact of the reservoir on the fluvial thermal regime is opposite. The images were atmospherically corrected using the In-Scene Atmospheric

Compensation algorithm implemented in the ENVI software [4]. The water surface temperature was calculated using the emissivity normalization method implemented in the same software [5] and considering a constant emissivity value of 0.985 for water.

Table 1. Remote sensing data.

Sensor	Platform	Date and time (GMT)	Location	Spatial resolution
ASTER	Terra satellite	11/09/2003, 10:53	Mequinenza and Ribarroja	90 m
ASTER	Terra satellite	5/03/2007, 11:01	Mequinenza and Ribarroja	90 m
TASI	Caravan aircraft	31/03/2011, 10:47-11:13	Mequinenza and Ribarroja	3 m
ASTER	Terra satellite	01/02/2002, 11:15	Sobrón	90 m
TIRS	Landsat 8	05/08/2014, 13:00	Sobrón	100 m

The TASI hyperspectral image was acquired during a survey flight over the confluence of the Segre River into the Ribarroja reservoir undertaken by the Institut Cartogràfic i Geològic de Catalunya on 31 March 2011. The TASI measurements were radiometrically corrected and spectrally aligned using the Radcorr and Speccorr tools, developed by ITRES, and the RadCaPP software, produced by the ICGC for residual errors compensation.

Water surface temperature was computed at every pixel as the value minimizing the summation of differences between the TASI radiance measurements and the Planck law's theoretical emission from the water surface plus the atmospheric contribution. This method provided a better fit to the in-situ values than the TES one [6] and than the average temperature resulting from the Planck's equation inversion for each band.

The ModTran 5.0 standard winter profile for medium latitudes [7] was used for the atmospheric characterization, together with the profiles provided by the National Center for Environmental Prediction (NCEP). The NCEP profiles were spatially and temporally interpolated to the study area central point and to the flight execution time [8]. The atmospheric radiance and transmissivity values for all TASI bands were computed using the Modtran 5.0.

##### *Sobrón reservoir*

Surface temperature in the Sobrón reservoir was derived from the ASTER image of 2 February 2002, following the same methodology as for the Mequinenza ASTER data.

Landsat 8 thermal data is acquired at 100 m resolution and distributed at 30 m, after cubic convolution

resampling. This resampling causes the land radiance to affect the thermal values of the water pixels near the reservoir banks. Given the narrowness of the Sobrón reservoir, many water pixels' radiance might be blurred by the resampling. The methodology as follows was developed in order to determine the appropriate water pixels for temperature retrieval: thresholding of the Normalized Difference Water Index was first applied to generate an open water mask for the Landsat images. The masks were resampled to 1 m spatial resolution and they were assigned two different DN values: one over water (DN=1) and another over land (DN=C), according to the maximum thermal contrast (C) between water and river banks in the original image. A Landsat 8 thermal image was simulated by resampling the modified water masks to 100 m resolution using the boxcar method. Cubic convolution was applied to resample again the latter image to 30 m resolution. Those water pixels whose values were altered by less than 5% (i.e. with values between 0.95 and 1.05) after the last resampling were selected for temperature retrieval.

Landsat images were corrected for atmospheric effects in order to retrieve the water leaving thermal radiance. The atmospheric radiance and transmissivity values for the Landsat 8 thermal band were computed using the Modtran 5.0 software and the NECP profiles interpolated to the Sobrón location [8].

### 3.2 Field data

#### *In Mequinenza and Ribarroja*

Vertical temperature profiles were acquired from a boat concurrently with the TASI flight survey. In-depth water temperatures were also collected at 10 minute intervals by a thermistor chain perched on a buoy in the centre of the Ribarroja reservoir [2].

#### *In Sobrón*

On 5 August 2014 at 13:00, a cloud free Landsat 8 image was acquired over the Sobrón reservoir, during the maximum thermal stratification period, and close to the daily water temperature peak time. A surface temperature acquisition campaign was undertaken in the reservoir between 10:30 and 14:30 on 7 August 2014, 48 hours after the acquisition of the Landsat 8 image over the site.

### 3.3 Thermo-hydrodynamic simulation model

#### *Mequinenza and Ribarroja*

Mixing phenomena occurring at the confluence of the Segre River, the Mequinenza discharge and the Ribarroja reservoir have a markedly three-dimensional dynamics. Thermal processes that took place throughout the day on March 31, date of the TASI sensor flight, were simulated using the finite volume, three-dimensional hydrodynamic model FreeFlow [9]. In addition to the water motion, this model simulates the

heat transfer within the fluid mass and the energy exchange with the atmosphere. Among the outputs are the temperatures at each volume element and time step of the simulated period [2].

Boundary conditions for the simulation included: water levels and flow discharges in the system, incident solar radiation and other meteorological variables.

#### *Sobrón*

The hydrodynamics of the Ebro River and Sobrón reservoir around the location of the cooling flow intake and discharge were also simulated using the FreeFlow modelling software.

## 4. 1.RESULTS AND DISCUSSION

#### *Mequinenza and Ribarroja*

Fig. 2 shows the water surface temperature map in the Mequinenza reservoir, derived from the ASTER image of 11 September 2003. Fig. 3 depicts the surface temperature profile along the fluvial axis, up to the Ribarroja reservoir tail.

The ASTER image was acquired in late summer, at a time of intense thermal stratification in the Mequinenza reservoir. When arriving into Mequinenza, the Ebro flow plunges beneath the warmer and less dense surface water of the reservoir. Fig. 2 and Fig. 3 reveal the river section in which this phenomenon occurs. The thermal profile of September 11 (Fig. 3) clearly shows the sharp increase in surface temperature at the point where the river hydrodynamics turn into the reservoir's. A gradual warming of the surface water is observed in Mequinenza reservoir in the downstream direction up to the vicinity of the dam, where a rapid decline occurs in the area affected by the turbines suction.

Right downstream of the dam, the water temperature is about 18 C. This value is indicative of the temperature at the bottom of the stratified mass or hypolimnion, from which the turbinated flow is extracted. The Segre River mouth and the Ribarroja tail can also be distinguished in Fig. 2 and Fig. 3, given their different surface temperatures.

Fig. 3 includes the longitudinal profile of surface temperature in Mequinenza derived from the ASTER image of 5 March 2007. In this case, the reservoir thermal impact is clearly different than at the end of the summer. The increasing solar radiation in March heats the Ebro River surface faster than that of the reservoir, given the greater thermal inertia of the latter. The Ebro flow, slightly warmer, stays on the reservoir surface. A temperature gradient declining downstream is observed, as opposed to the downstream warming to be expected in absence of reservoirs.

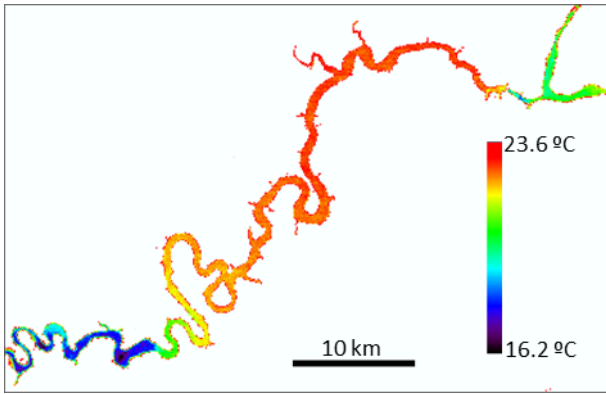


Figure 2. Water surface temperature in the Mequinenza reservoir, obtained from the ASTER image of 11 September 2003.

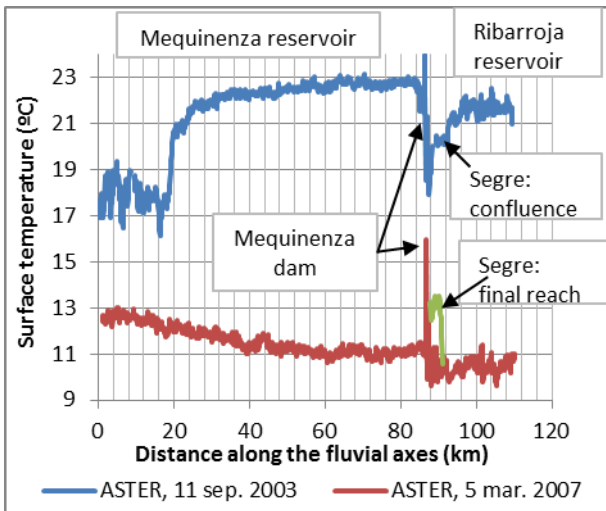


Figure 3. Water surface temperature along the fluvial axis, obtained from two ASTER images for the reach represented in Fig. 2.

Fig. 4.a presents the surface temperature map in the Ribarroja tail, derived from the TASI survey flight on 31 March 2011. The excellent spatial resolution of this map enables the observation of spatial mixing patterns, such as the Kelvin-Helmholtz instabilities along the contact between the waters from Mequinenza and the Segre tributary. The detailed temperature map, along with the vertical temperature profiles were used for the validation of the 3D thermo-hydrodynamic model of this site [2].

Fig. 4.b shows the results of the thermo-hydrodynamic model at the simulation time of the TASI acquisition. The simulated temperatures adequately resembled the in-situ thermal profiles. However, the reduced number of in-depth profiles that could be collected at the approximate time of the TASI overflight was insufficient for characterizing the accused spatial thermal gradients occurring in the site. The TASI's high resolution, spatially continuous data was of great

relevance to assess the model's performance.

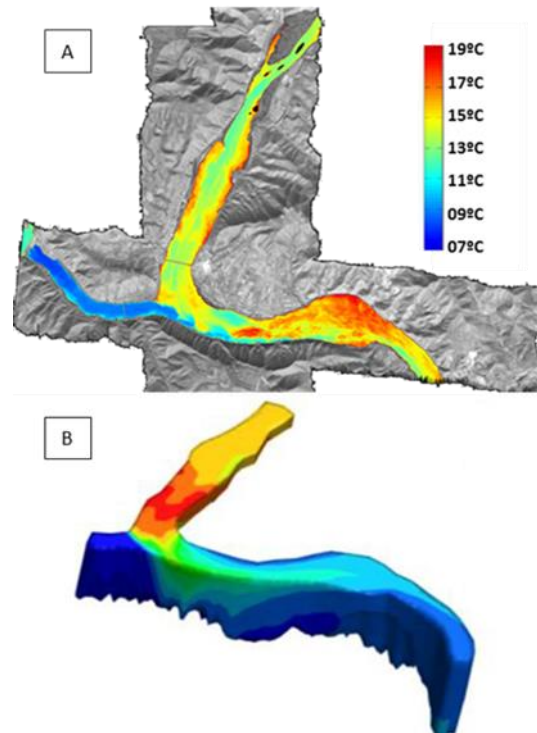


Figure 4. Water temperature in the Ribarroja reservoir tail on 31 March 2011, 11:00 GMT: a) surface temperature obtained from the TASI survey flight; b) temperature in the reservoir volume simulated with the FreeFlow modelling tool.

#### Sobrón

Water surface temperatures derived from the Landsat 8 image from 5 August 2014 showed a root mean squared error of 0.6 C when compared to the in-situ temperatures measured +20 minutes off the image acquisition time. The error increases with the time shift between image and in-situ measurements, since the high solar radiation was heating the reservoir surface rapidly.

The ASTER image from 1 February 2002 revealed an abrupt increase in surface temperature at the location of the nuclear power plant's cooling flow discharge (Fig. 5). According to the retrieved thermal profile, the discharge seems to affect the river surface temperature along approximately 5 km upstream. Preliminary numerical simulations of the site thermo-hydrodynamics showed a similar backwater effect of the cooling flow discharge, increasing the upstream river surface temperature.

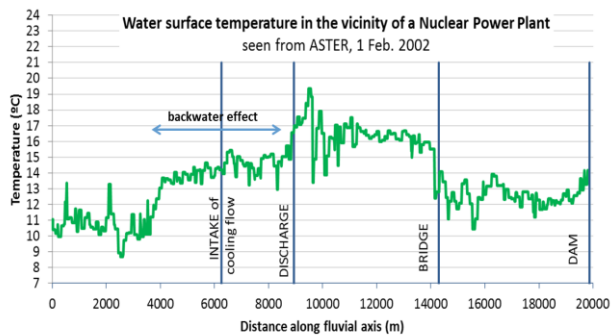


Figure 5. Water surface temperature of the Ebro River and Sobrón reservoir derived from the ASTER image of 1 Feb. 2002.

## 5. CONCLUSIONS

The spatially continuous water surface temperatures retrieved from remote sensing data over large areas provide an exclusive insight into the river and reservoir thermo-hydrodynamics, complementing the information from in-situ measurements. According to this study's results the thermal mapping derived from satellite imagery can reveal:

- The reservoir impact on the river longitudinal temperature gradient at different times of the year.
- The initial cross section of the thermal stratification and its temporal evolution.
- The extent of the surface cooling in the vicinity of the dam, due to the vertical mixing induced by the hydro-electrical turbines intake.
- The uneven heating of the reservoir surface.
- The impact of a nuclear power plant cooling flow on the river temperature profile.

The high spatial resolution of the TASI airborne data enabled the detailed observation of mixing phenomena in the tail of the Ribarroja reservoir and provided valuable spatial data for validating the 3D thermo-hydrodynamic model of the water body.

## 6. REFERENCES

1. Prats, J. (2011). *El règim tèrmic del tram inferior de l'Ebre i les seues alteracions*, PhD dissertation, Barcelona: Universitat Politècnica de Catalunya, 331 pp.
2. Arbat-Bofill, M. (2015). *Distribución de temperatura y velocidad en embalses. Análisis numérico-experimental aplicado a los embalses de Sau (Ter) y Ribarroja (Ebro)*. PhD dissertation, Barcelona: Universitat Politècnica de Catalunya, 412 pp.
3. Prats Rodríguez, J., Val Segura, R., Arbat-Bofill, M., Martí-Cardona, B., Ninyerola Chifoni, D., Armengol Bachero, J., & Dolz Ripollés, J. (2015). Trabajos de seguimiento de la temperatura del agua en el curso inferior del río Ebro, España. In

Proc. 1<sup>er</sup> Congreso Iberoamericano sobre Sedimentos y Ecología, Querétaro, México, 21-24 Jul.

4. Johnson, B. R. & Young, S. J., (1998). In-Scene Atmospheric Compensation: Application to SEBASS Data Collected at the ARM Site, Technical Report, Space and Environment Technology Center, The Aerospace Corporation.
5. Hook, S. J., Gabell, A. R., Green, A. A. & Kealy, P. S. (1992). A comparison of techniques for extracting emissivity information from thermal infrared data for geologic studies, *Remote Sensing of Environment* **42**, 123-135.
6. Gillespie, A. R., Rokugawa, S., Hook, S., Matsunaga, T. & Kahle, A. B. (1998). A temperature and emissivity separation algorithm for Advanced Spaceborne Thermal Emission and Reflection Radiometer (ASTER) images, *IEEE Transactions on Geoscience and Remote Sensing* **36**, 1113-1126.
7. Berk A. et al. (2005). MODTRAN 5: A Reformulated Atmospheric Band Model with Auxiliary Species and Practical Multiple Scattering Options: Update, Proceedings of the SPIE, **5806**, 662-667.
8. Barsi, J.A., J.L. Barker & J.R. Schott (2003). An Atmospheric Correction Parameter Calculator for a Single Thermal Band Earth-Sensing Instrument. IGARSS03, 21-25 Jul., Centre de Congres Pierre Baudis, Toulouse, France.
9. Cea, L., Stelling, G. & Zijlema, M. (2008). Non-hydrostatic 3D free surface layer-structured finite volume model for short wave propagation, *International Journal for Numerical Methods in Fluids* **61**, 382-410.